Application of linear prediction and singular value decomposition for the analysis of periodic oscillations in coherent excitation spectra of condensed media and solid interfaces

2010 J. Phys.: Condens. Matter 22 084015

(http://iopscience.iop.org/0953-8984/22/8/084015)

IOP Publishing Journal of Physics: Condensed Matter

J. Phys.: Condens. Matter **22** (2010) 084015 (7pp) doi:10.1088/0953-8984/22/8/084015

Application of linear prediction and singular value decomposition for the analysis of periodic oscillations in coherent excitation spectra of condensed media and solid interfaces

D Hoogestraat and K Al-Shamery

Physical Chemistry 1, Institute for Pure and Applied Chemistry, Carl von Ossietzky University of Oldenburg, 26129 Oldenburg, Germany

E-mail: d.hoogestraat@uni-oldenburg.de

Received 1 July 2009, in final form 21 September 2009
Published 4 February 2010
Online at stacks.iop.org/JPhysCM/22/084015

Abstract

The observation of periodic responses after absorption of ultrashort laser pulses in condensed media and at solid interfaces is a common phenomena in various time-resolved spectroscopic methods using laser pulses shorter than the period of the coherently excited vibrations. Normally these signals have to be separated from strong slowly decaying backgrounds related to the creation of nonequilibrium carriers. The recording normally requires either a small period of time or lacks temporal resolution to obtain the good signal-to-noise ratio necessary for the observation of the vibrations. The standard method used for the analysis of the data is a curve-fitting routine to the time-domain data. However, the disadvantage is the necessity to estimate the number of spectral components before fitting. This paper will introduce under which conditions linear prediction and singular value decomposition in combination with an iterative nonlinear fitting in the time and spectral domain may extract an unknown number of spectral components including amplitude, lifetime, frequency and phase. Such information is essential to unambiguously evaluate the dominant optical excitation process, the phase of the initial displacement, the symmetry of the excited vibrational mode and the specific vibration generation process.

(Some figures in this article are in colour only in the electronic version)

1. Introduction

In the last few years, many time-resolved vibrational spectroscopy experiments were carried out, using ultrafast lasers in combination with pump probe techniques. Commonly, in those experiments the pulses from a laser source are split up by means of a interferometric set-up resulting in a pump pulse to excite the sample under investigation (such as stimulation of vibrational modes in lattices or adsorbates) and a second, delayed pulse to interrogate the sample's response. By scanning through different delays, one can retrieve complete information about the dynamics on a femtosecond timescale. Depending on the sample, the excitation pulse is creating a nonequilibrium carrier distribution which directly affects optical properties such as reflectivity, absorption or the second-order nonlinear susceptibility $\chi^{(2)}$. In this way acoustic breathing mode vibrations of colloidal gold particles [1] and metallic nanoprisms [2, 3], acoustic phonons in bismuth films on silicon [4] and interface phonons on GaAs semiconductor substrates [5–8] were investigated.

The signal intensities and signal-to-noise ratios (SNR) are rather small. For example, in reflectivity measurements on GaAs surfaces the response due to carrier excitation is of the order of 10^{-4}, the phonon signal in the range of 10^{-5} of the overall reflectivity signal [9, 10]. This requires, beside

being meticulous in reducing noise sources [11], averaging over many scans. As an accompaniment, either the recorded data spans only a small period in time or it lacks temporal resolution. This, of course, directly affects the analysis, normally accomplished by a fast Fourier transformation of the apodized data. The resulting problems are spectral distortions, depending on the apodization function used and the risk of peak overlapping (the resolution is approximately the inverse of the signal length).

To overcome this limitation a standard procedure is to apply a curve-fitting routine to the time-domain data. As a consequence of the nature of the underlying model, a nonlinear method has to be used, which needs preferably a good set of starting parameters to convolute to a solution. So the number of spectral components has to be estimated before fitting.

In this paper we want to introduce the use of the linear prediction singular value decomposition (LPSVD) method, which is a linear routine, in combination with an iterative nonlinear fitting in the time and spectral domain to extract spectral components. The LPSVD was introduced by Kumaresan and Tufts [12] and is used in NMR spectroscopy to analyze the free induction decays (FID) in pulsed measurements, in particular in *in vivo* experiments with low SNR [13, 14]. To demonstrate the LPSVD and the complete fitting procedure, we apply it to simulated data and to results from phonon studies on GaAs(100) using time-resolved second harmonic generation (TRSHG) experiments done in our group. The latter we compare to results known from the literature [5, 6, 8, 9, 15–17]. The advantage of using this method is that even complex spectral responses can be analyzed without presuming the number of components and a far better resolution can be obtained in comparison to normally used routines in coherent laser experiments. In the first section the experimental set-up, the software packages used and the raw results are shown. An initial step which does not occur in NMR data is the need to separate the phonon signal from the electronic background prior to further processing. This part will be discussed in the second section before the LPSVD and the whole fitting procedure is explained in the third section. Processing of simulated experimental data is shown in the following two sections.

2. Experiment and software

2.1. Set-up

For the TRSHG experiments a KML oscillator with a repetition rate of 95 MHz was used. It delivers pulses with a duration around 35 fs and a central wavelength tunable between 1.47 and 1.59 eV (780–840 nm). In a Mach–Zehnder interferometer the pulses were split up in a 80:20 ratio, resulting in a pump beam with 130 mW, which was chopped and focused on the sample in a spot of 80 μm. The weaker probe beam ($\sim$30 mW) was delayed by a translational stage and focused noncollinearly on the same spot on the sample. After blocking the fundamental by means of color and interference filters the probe signal was detected with a cooled Hamamatsu photomultiplier tube, fed into a FEMTO lock-in amplifier and digitalized by a National Instruments AD converter. By using wave plates and polarizers in the pump, probe and detection beam it is possible to access the various tensor elements of the nonlinear polarization source $P^{\mathrm{NL}}(2\omega)$.

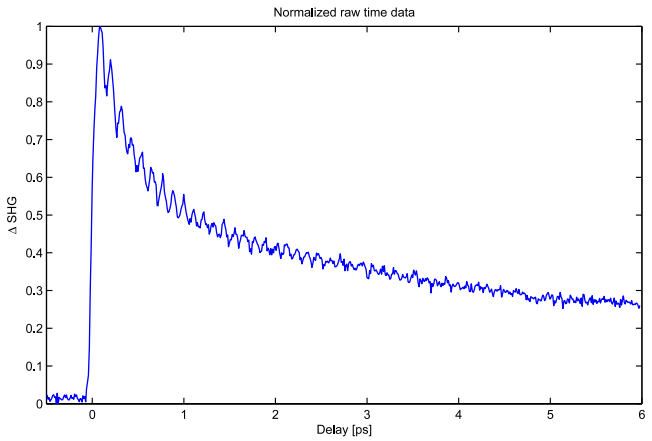

Figure 1. Average over 50 scans in p-polarized probe and detection beam, s-polarized pump configuration of a native-oxide-covered GaAs(100) sample along the [0$\bar{1}$0] direction.

A GaAs wafer in (100) orientation was obtained from CrysTec. To remove the protective coating and residues from processing it was cleaned by ultrasonication in acetone and isopropyl alcohol. This clean, but still oxide-capped crystal, was mounted on a rotational stage, which allowed us to scan different crystal directions. Figure 1 shows the normalized time signal retrieved by averaging over 50 scans with 10 fs sampling interval. In this measurement the incoming probe and detection beam were p-polarized, whereas the polarization of the pump beam was rotated about 90° to s-polarization. The sample was aligned along the [0$\bar{1}$0] direction.

2.2. Software

For controlling the experiment and recording the data a self-written *C*♯ program was used. *Matlab*® (R2008b, The MathWorks, Natick, USA) with *Optimization*, *Curve Fitting* and *Signal Processing* toolboxes was used to process data. The LPSVD routine was extracted from the *matNMR* (Version 3.9.59, JD van Beek) package [18].

3. Separation of background and data processing

As shown in figure 1 the initial carrier excitation response and the phonon signal completely overlap temporally. When information about modes with short lifetimes or the initial phase of a vibration is needed, the separation of both signals is to be conducted carefully. While the decay can be modeled by a biexponential function with the two decay times addressed to electron–electron and electron–phonon scattering [19], particular attention has to be paid to the initial rising edge of the signal in the zero delay area and the first period of the oscillation around 150 fs. Due to coherent coupling between the pump and probe pulses the signal can be distorted within the period of the pulse width [20, 21].

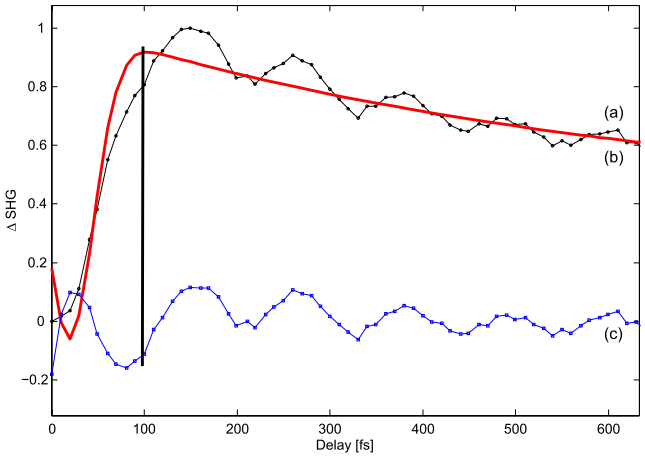

Figure 2. Raw data (a), fit (b) and subtracted phonon signal (c). The data will be cut at the peak of the fit at 100 fs. A bad overlap of the fit and the data at delay times <100 fs will lead to additional oscillations, as can be seen easily.

The shape of this distortion is, depending on the laser pulse, Gaussian, Lorentzian or sech^2. Hence the first oscillation period could also be attributed to an overshot in the signal due to convolution of the biexponential function with the coherent coupling. Furthermore this distortion complicates the determination of the starting point of the oscillatory part, which is very important in order to understand the underlying excitation mechanism. Details about handling of this problem will be discussed elsewhere. As the scope of this paper is the use of the LPSVD method, we will, without further discussion, fit the data signal to a combination of a biexponential and a Gaussian with the width fixed to the pulse duration of 38 fs according to our autocorrelation analysis of our laser beam. As shown in figure 2 the data is cut at the peak position of the fit at 100 fs. The oscillation period at delay times <100 fs is due to a bad overlap of fit and data, for the reasons stated above.

After subtraction a locally weighted scatter plot smoothing (LOWESS), using a least-squares fitting and a first-order polynomial, is applied to the data to reduce low frequency components (<1 THz). After that an apodization equation (1) is applied and a zero filled fast Fourier transformation (FFT) is performed. The apodization function is chosen to be the same as in [9], for which no apodization effects have to be considered when comparing the two results:

$$A(t) = \cos\left(\pi/2 \cdot \frac{t - t_0}{t_{\text{end}} - t_0}\right). \tag{1}$$

For the fitting routine two datasets are used: the apodized time signal and the concatenated imaginary and real part of the Fourier transform.

4. LPSVD routine and fitting procedure

For the LPSVD method and the iterative fit, the oscillations are modeled by a sum of N damped complex sinusoids plus white noise $w(t)$:

$$S(t) = \sum_{n=1}^{N}\left[\alpha_n \cdot \exp\left(-\frac{1}{\tau_n}\cdot t + \mathrm{i}2\pi f_n \cdot t\right)\right] \cdot w(t) \tag{2}$$

where $n = 1, 2, \ldots, N$, α_n is the complex amplitude describing the real amplitude a_n and the phase ϕ_n, τ_n is the damping time and f_n the frequency. Thus fitting this model to experimental data involves $4N$ variables, where N is unknown and has to be carefully estimated. Also a good set of starting parameters is needed.

4.1. LPSVD

The LPSVD method uses linear prediction, either in the forward or backward direction. The idea is to assume that any data point in the equally spaced data ($i\Delta t; i \in \mathbb{N}$) can be expressed by its preceding or following points. Equation (3) expresses the relation for the backward prediction, where q_n is the n th prediction coefficient and M is the number of data points accounted for in the prediction:

$$s_i^{\text{predicted}} = \sum_{n=1}^{M} q_n s_{i+n}. \tag{3}$$

It can be shown that for a signal consisting of N noise-free oscillations $M = 2N$ data points have to be included in the prediction, so there are also $2N$ prediction coefficients [12, 22]. In the presence of noise, this number is increasing.

The prediction parameters can now be fitted to the data in a linear fashion, without specifying any start values. In the approach by Kumaresan and Tufts [12] singular value decomposition (SVD) is used to obtain the parameters. For this, a Hankel matrix has to be created by taking the dataset consisting of K points and arranging it in M columns and $K - M + 1$ rows in such a way that every row is filled with values $s_{1+c}, \ldots, s_{M+c}$, where c is the zero-based row index (4):

$$H = \begin{pmatrix} s_1 & s_2 & \cdots & s_M \\ s_2 & s_3 & \cdots & s_{M+1} \\ \vdots & \vdots & & \vdots \\ s_{K-M+1} & s_{K-M+2} & \cdots & s_K \end{pmatrix} \tag{4}$$

M has not to be known and can be chosen by roughly estimating the number of oscillations and concerning $M = 2N$. Another guideline is trying to make the matrix as square as possible. The linear prediction can now be expressed with this matrix by a combination of (3) and (4), using complex conjugate data:

$$\overline{s} = H \cdot \overline{q} \tag{5}$$

where $\overline{s}$ and $\overline{q}$ are vectors with dimensions $K - M + 1$ and M. The next step is to factorize the Hankel matrix H into three matrices:

$$H = U \cdot S \cdot V' \tag{6}$$

U and V' are a unitary matrix and the conjugate transpose of a unitary matrix, containing the left and right side singular vectors, respectively. S is a diagonal matrix, with positive values in descending order. Those values are equal to the

square roots of the eigenvalues obtained from $H \cdot H'$. For an ideal noise-free signal the rank of matrix S is equal to the number of prediction coefficients, hence $2N$. With increasing noise the number of non-zero elements is also increasing, but they can be easily identified and separated as long as a critical SNR has not been reached. A common approach is to use Cadzow filtering to remove noise components and is presented in [23].

After reducing S one can create an inverted Hankel matrix by performing

$$\mathrm{inv}(H) = V \cdot \mathrm{inv}(S) \cdot U' \tag{7}$$

and use this to calculate the prediction coefficients by separating $\overline{q}$ in equation (5). The last step is to convert the prediction coefficient to the wanted oscillation parameters. While the damping times and frequencies can be directly calculated, the amplitudes and phase information have to be obtained by another linear square procedure after inserting the extracted damping times and frequencies into the model signals [22].

4.2. Fitting procedure

Before the LPSVD is applied to the apodized time data, some spectral bandpass filtering has to be considered. Our 6 ps long experimental dataset from figure 1 is sampled with 10 fs and therefore has a Nyquist length of 50 THz and a resolution of about 0.16 Thz. But, due to the coherent excitation mechanism, it is not possible to excite modes with frequencies higher than that of the pump pulse. This leads to an upper frequency limit of 20 THz, in a careful approach by taking the autocorrelation pulse width of 50 fs into account. Also the low frequency side of frequencies smaller than 3 THz tend to be noisy, in particular residual electronic excitation components in the signal, which could not be completely removed by the background fit, may appear as non-physical ghost frequencies. By excluding these areas, the performance of the fitting can be improved.

After the filtering LPSVD is applied to analyze the oscillatory components. In the next section two different cases are presented. On the one hand, we apply Cadzow filtration to reduce the diagonal matrix S received from the SVD, while, on the other hand, we just estimate a large number of oscillations ($M = 20$) and let the routine calculate their parameters, even from those which originate from noise, to show that these noise signals can also be identified in the final LPSVD results.

In the last step these parameters are fed into the iterative routine. This routine is a method commonly used [9, 15], but mostly not described in detail. The idea is to fit the $4N$ parameters resulting from the LPSVD procedure iteratively to the time and frequency domain. Therefore the frequencies and lifetimes are kept constant and the amplitudes and phases are fitted in a nonlinear least-squares sense to the apodized time data by using an apodized form of (2). The optimized amplitudes and phases are then fixed parameters in the following fit of the frequencies and lifetimes to the concatenated imaginary and real parts of the FFT spectrum. Overall around ten to a thousand complete circles are performed, depending on the complexity of the signal. By comparing the apodized time signal with an also apodized model, the effect of apodization should be completely removed [9].

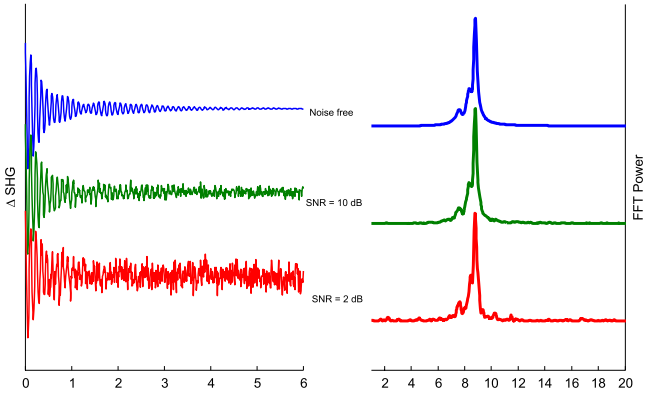

Figure 3. Example of time data and corresponding power spectra of model signal for three different SNR levels.

5. Application to modeled data

In order to elucidate the sensitivity of the result obtained with our fitting (LPSVD) routine to the SNR of the experimental data, we shall first discuss model data containing three oscillatory components similar to those expected in real experiments on oxide-covered GaAs surfaces. We shall omit steps related to extraction of the background signal and removing low frequency components in these tests. To investigate the effect of noise on the retrieval of oscillatory components, model signals with increasing amounts of Gaussian white noise are created (figure 3), based on the parameters shown in the first three rows in table 1. The noise is specified as SNR in dB units.

For the noise-free signal the parameters are perfectly restored: the S matrix consist of six non-zero elements, resulting in six oscillations where half of them differ just by the sign of the frequency and thus are to be neglected.

Also for the 100 dB signal all components are extracted without any special reduction of the S matrix. Only the phase exhibits slight shifts. When applying the LPSVD without any filtering to the 30 dB sample it results in the parameters shown in table 2. Here the real features are still well retrieved but there are additional components induced by the noise. With this noise level they can still be removed by looking at their small amplitudes and comparably high lifetimes. To remove those components directly inside the LPSVD routine the above-mentioned Cadzow filtration can be applied. For this the values of singular values are drawn in figure 4. The diagonal matrix will now be reduced by rejecting all values with indices larger than that at the center of the last rising edge. The results of this step are also shown in table 1. With further increasing noise the step edge between real oscillations and noise starts to vanish. More noise signals will enter the LPSVD results and the quality of the retrieved parameters decreases, especially of those close to the noise edge. Now the second step in the fitting procedure, the iterative step, is taken into account. The results

Table 1. Parameters for the model signals taken from real results from native-oxide-covered GaAs(100) [9] and results for the noisy model signals retrieved by applying LPSVD only.

SNR (dB)	Amplitude	Damping time (ps)	Frequency (THz)	Phase
∞	220	1.4	8.76	0
	300	0.57	8.36	0
	100	0.72	7.65	0
100	220	1.39	8.76	6.6×10^{-6}
	300	0.57	8.35	1.2×10^{-5}
	110	0.72	7.65	8.1×10^{-6}
30	220.8	1.39	8.76	0.01
	303	0.57	8.36	0.02
	106	0.74	7.65	0.02
10	216	1.48	8.75	0.02
	299	0.63	8.33	0.18
	156	0.55	7.7	0.20
	6.14	0.59	6.83	1.17
	⋮	⋮	⋮	⋮
2	224	1.54	8.71	0.52
	302	0.85	8.53	0.52
	107	1.12	7.61	0.17
	⋮	⋮	⋮	⋮

Table 2. Raw LPSVD results for the 30 dB model signal. The negative frequency components are already removed.

Amplitude	Damping time (ps)	Frequency (THz)	Phase
220	1.39	8.76	0.01
304	0.56	8.35	−0.03
112	0.68	7.65	0.03
0.94	2.55	4.9	1.78
0.38	9.93	3.91	−1.58
1.54	1.56	3.8	1.98
0.38	8.92	4.3	2.0

for this step are presented in table 3 for the 10 and 2 dB signals. It is obvious that the restored oscillations are derived from the original parameters. The noise signals reach higher amplitudes and become more difficult to distinguish from real signals, even though the iterative fit in combination with the LPSVD nicely convolutes to the noisy data as seen in figure 5.

6. Application to GaAs TRSHG experiments

Now we want to apply the routine to an experimental dataset, which was measured in our group shown in figures 1 and 2. The sample consists of a native-oxide-layer-covered GaAs(100) crystal with Te n-doping (2×10^{18} cm^{-3}). The further processing of this data was presented in previous sections. Here we want to apply the LPSVD method with Cadzow filtering and the iterative fit. As seen in figure 6 the transition from noise to signal components is again not sharp. So we chose a larger number of singular values to remain in the diagonal matrix S so as not to accidentally remove signal components. This leads to the signals shown in the first rows of table 4, from which three seem to be real signals and the

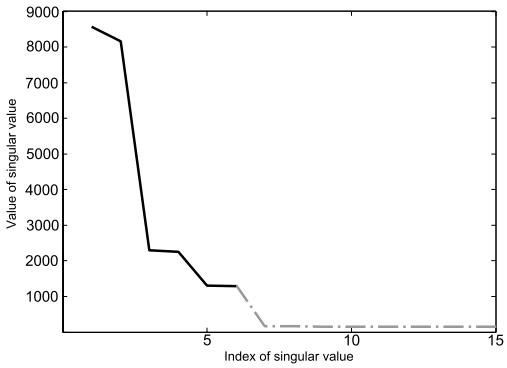

Figure 4. Singular values of the 30 dB model signal.

Table 3. Results for the noisy model signals retrieved by applying LPSVD and the iterative fit.

SNR (dB)	Amplitude	Damping time (ps)	Frequency (THz)	Phase
10	225	1.41	8.75	0.01
	283	0.64	8.35	0.13
	156	0.56	7.66	−0.02
	7.8	1.3	11.43	1.96
	19	0.84	6.87	−1.32
	3.14	9.34	9.96	2.03
2	137	2.15	8.71	0.82
	378	0.72	8.54	−0.22
	139	0.83	7.63	0.04
	24	2.9	10.27	−0.32
	44.1	3.26	9.13	−2.47
	⋮	⋮	⋮	⋮

others may arise from noise. The iterative fit of the data is summarized in the lower rows of the same table. Chang extracted three components in his work on a similar sample with frequencies, amplitudes and damping times as shown in the first rows of table 1 [9, 5]. He assigned the mode at 8.8 THz to the LO bulk mode, while the 7.65 THz oscillation was attributed to the LO bulk and electron-plasma-coupled mode at the back of the depletion region. Finally in [9] the mode around 8.65 THz was described as a Fuchs–Kliewer oscillation, which was later [5] corrected to a not further specified surface confined mode in the top four layers of the sample. If we compare this to the results from the first LPSVD step we find a good agreement for the 8.8 and 7.65 THz modes. The low amplitude and elevated damping time of our mode at 8.48 THz makes it suspicious. Normally this combination is a sign of a noise-contributed signal or at least a very weak signal which is buried in noise. The phases of these modes are all in the same range. An absolute determination of the phase is not possible without a reference.

The iterative fit convolutes very well to the spectral and time signal, but the resulting parameters are in less agreement with the results from Chang and those received by the pure LPSVD routine. In particular, the damping times of the LO bulk and the electron-plasma-coupled mode are decreased. An exception is the damping time of the uncertain 8.45 THz mode

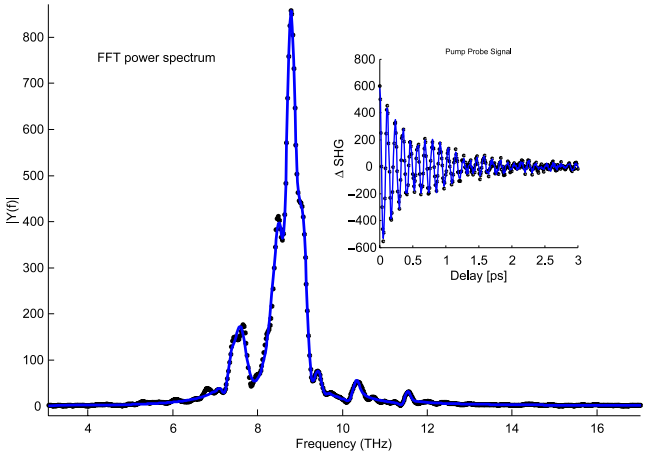

Figure 5. Fit in the time and spectral domain to the noisy signal of 2 dB.

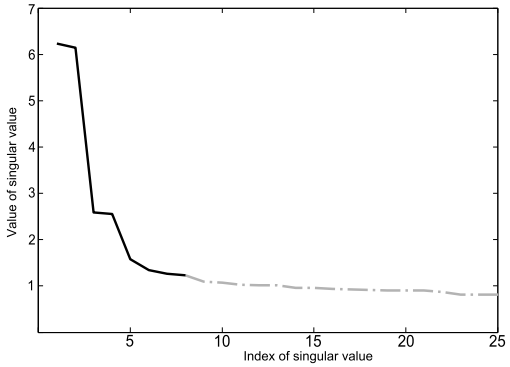

Figure 6. Singular values for the experimental dataset.

which is further increased. Finally a high frequency component at around 9.3 THz is newly found.

7. Summary and conclusion

In this paper we discussed the advantages and limitations of using a combination of linear prediction singular value decomposition (LPSVD) with an iterative fitting method for the analysis of time-resolved phonon spectroscopy experiments. The key benefit of using LPSVD is that it delivers the number of oscillatory components contained in the analyzed signal without any *a priori* knowledge about the system. By concatenation of this method with an iterative nonlinear curve fitting to the temporal and spectral domains one can extract full spectroscopical data even from complex signals. The LPSVD is used to supply starting points for the nonlinear method, which depends on a good set of starting parameters and a predetermined number of oscillations. As an example we chose a time-resolved second-harmonic-generation-based phonon spectroscopy experiment on GaAs samples, for which a number of not very well separated surface and bulk phonon modes can be found. To test the method, simulated datasets consisting of three phonon modes and white noise were generated. We employed our method on these data and varied the noise level. For

Table 4. Results for the experimental data using LPSVD with Cadzow filtration (upper rows) and after application of fitting routine (lower rows).

Method	Amplitude	Damping time (ps)	Frequency (THz)	Phase
LPSVD	0.099	1.51	8.80	2.6
plus	0.02	3.55	8.48	2.79
Cadzow	0.045	0.56	7.56	2.96
	0.005	1.94	9.8	−0.93
	0.003	5.1	7.46	0.51
LPSVD	0.45	0.70	8.88	−3.02
plus	0.03	7.49	8.51	1.74
it. fit	0.14	0.35	7.68	2.3
	0.19	0.44	9.28	−0.53
	0.068	0.2	6.9	0.27

signals down to 10 dB the spectral components can be extracted from the LPSVD method directly. For data with a higher fraction of noise Cadzow filtration inside the diagonal matrix and the second iterative fitting step become more important.

Next a real pump probe trace from experiments on n-doped GaAs(100) crystals done in our workgroup was analyzed. This signal is more complex due to the fact that not only the vibration of the lattice contributes to the change in second-order susceptibility, but also the hot carriers affect the SHG response. The latter effect is even stronger by a factor of ten and has to be deconvoluted from the signal before analyzing. Beside that, the low signal-to-noise ratio requires averaging over many scans; consequently the recorded temporal window is small. Here the transition from real to noise components is not as sharp as in the simulated signals. Therefore a larger number of components is accepted in the Cadzow filtration step to avoid cutting potential important information. The fitting routine nicely reproduces the experimental dataset in the spectral and time domains. The LO bulk phonon mode at around 8.7 THz and the electron-plasma-coupled mode at 7.6 THz could also be found in our measurements within the resolution limit of 0.16 THz, both showing slightly smaller lifetimes as described by Chang [9]. The surface-related mode at 8.5 THz, found by Chang [5] is somewhat unclear due to its small amplitude and quite large lifetime. Additionally a new, and until now unreported, mode at around 9.3 THz is clearly visible in the spectrum and is also found by the fitting routine. An absolute determination of the phases is not possible without reference; however the phases of all signals relative to each other can be obtained.

In conclusion the combination of both fitting methods improves the fitting of complex data from time-resolved vibrational measurements. Even though at small signal-to-noise ratios it doesn't convolute to a noise-free solution, by looking at the singular values one gets a good measure for the quality and importance of every single component. It has also been demonstrated that even close lying modes can be revealed.

Acknowledgments

KA-S is grateful to the State of Lower Saxony and the German Science Foundation (DFG) for providing the money for the femtosecond laser system. Thanks go to Peter Clawin and Lars Schütte for helping to finalize the manuscript.

References

[1] Hodak J, Martini I and Hartland G 1998 *J. Chem. Phys.* **108** 9210
[2] Huang W, Qian W and El Sayed M 2005 *J. Phys. Chem.* B **109** 18881
[3] El-Sayed M, Qian W and Huang W 2004 *Nano Lett.* **4** 1741
[4] Hase M, Mizoguchi K, Harima H, Nakashima S, Tani M, Sakai K and Hangyo M 1996 *Appl. Phys. Lett.* **69** 2474
[5] Chang Y, Xu L and Tom H 1999 *Chem. Phys.* **251** 283
[6] Chang Y, Xu L and Tom H 1996 *Phys. Rev. Lett.* **78** 4649
[7] Cho G, Kütt W and Kurz H 1990 *Phys. Rev. Lett.* **65** 764
[8] Watanabe K, Dimitrov D, Takagi N and Matsumoto Y 2002 *Phys. Rev.* B **65** 235328
[9] Chang Y 1996 Study of coherent surface phonons using time-resolved second-harmonic generation *PhD Thesis* University of California, Riverside
[10] Dekorsy T, Pfeifer T, Kütt W and Kurz H 1992 *Phys. Rev.* B **47** 3842
[11] Oak S, Chari R and Vijayaragavan A 2005 *Indian J. Pure Appl. Phys.* **44** 330
[12] Kumaresan R and Tufts D 1982 *IEEE Trans. Acoust. Speech Signal Process.* **30** 833
[13] Lin Y, Hodgkinson P, Ernst M and Pines A 1997 *J. Magn. Reson.* **128** 30
[14] Barkhuijsen H, De Beer R, Bovee W, Creyghton J and Van Ordmondt D 1985 *Magn. Reson. Med.* **2** 86
[15] Levinsohn N, Beserman R, Cyternabb C, Brener R, Khait Y, Regei G, Musolf J, Weyers M, Brauers A and Balk P 1990 *Appl. Phys. Lett.* **56** 1131
[16] Tom H, Chang Y and Kwak H 1998 *Appl. Phys.* B **68** 305
[17] Tom H, Xu L and Chang Y 1999 *Phys. Rev.* B **59** 12220
[18] van Beek J 2007 *J. Magn. Reson.* **187** 19
[19] Shah J 1978 *Solid-State Electron.* **21** 43
[20] Sjodin T, Li C, Petek H and Dai H 2000 *Chem. Phys.* **251** 205
[21] Sjodin T, Petek H and Dai H 1998 *Phys. Rev. Lett.* **81** 5664
[22] Barkhuijsen H, De Beer R, Bovee W and Van Ormondt D 1985 *J. Magn. Reson.* **61** 465
[23] Cadzow J 1988 *IEEE Trans. Acoust. Speech Signal Process* **36** 49